



ISSN 0975-413X
CODEN (USA): PCHHAX

Der Pharma Chemica, 2016, 8(10):259-273
(<http://derpharmachemica.com/archive.html>)

Synthesis, Molecular Docking and evaluation of Antiangiogenic activity and Cellular metastasis potential of some Triazine and Pyrrolidin-2-one derivatives

^aAnkit Kumar, ^aUmesh Kumar Singh, ^bPratibha Gupta, ^aFaizi Muzaffar, ^aPrateek Pathak and ^cPraveen Kumar Tomar

^aKharvel Subharti College of Pharmacy, S. V. Subharti University, Meerut, UP, India

^bMahatma Gandhi Chitrakoot Gramoday Vishwavidyalaya, Chitrakoot, MP, India

^cDepartment of Chemistry, Zakir Husain Delhi College, University of Delhi, J. L. Nehru Marg, New Delhi, 110002, India

ABSTRACT

1,2,4-Triazine and Pyrrolidin-2-one derivatives with 1, 4 substituted salicylaldehyde were designed and synthesized in order to obtain new compounds with potential anticancer activity. The structures of all synthesized compounds were confirmed by means of spectroscopical analytical techniques. All compounds were evaluated for their anti-angiogenic activity and cells invasion and metastasis potential by chorioallantoic membrane (CAM) assay method. Compound 2b, 2c and 4d showed maximum antiangiogenic activity out of all synthesized compounds. Molecular docking studies of most active compounds of the series revealed that they bind to a narrow hydrophobic pocket of the N-terminal chain in the ATP binding site of VEGFR.

Key words: Angiogenesis, triazine, pyrrolidin-2-one, CAM assay, VEGFR.

INTRODUCTION

Cancer is the second frequent cause of human death in the world with 11 million new incidences every year. It is responsible for one in eight deaths worldwide. There are more than 100 distinct types of cancer originating from most of the cell types and organs throughout the human body. Cancer is characterized by relatively uncontrolled proliferation of cells escaping from apoptosis that can invade beyond normal tissue boundaries and metastasize to distant organs. Cancer cells grow and divide much more rapidly than normal cells so that they have a much higher demand for nutrients and oxygen. Angiogenesis (growing blood vessels network) provides nutrition for the growth of tumors, growing tumor invade in to the adjacent tissues (metastasis). Cancer cells cannot grow into noticeable tumors without sufficient amounts of capillaries feeding them oxygen- and nutrient-rich blood. Angiogenic inhibitors are a new class of anticancer drugs which act by inhibiting nutrition carriers (blood vessels growth) of tumors. Angiogenesis inhibitors are unique cancer-fighting agents because they inhibit the growth of blood vessels rather than tumor cells or prevents tumor from growing. The FDA has been approved angiogenesis inhibitors for cancer treatment including sorafenib, sunitinib, pazopanib and everolimus. Various types of angiogenesis inhibitors are currently being tested in clinical trials. We use starve to kill approach (inhibition of angiogenesis a nutrition path to cancer cells) to fight with cancer. Triazine has wide pharmacological properties like anticancer, antiviral,

antibacterial, antifungal, antiprotozoal, anti-inflammatory and antidepressant. Pyrrolidin-2-one has been reported to have anti-inflammatory, anticonvulsant and protein kinase inhibition potential. [1-6]

CAM assays have been extensively used to study angiogenesis [2], tumor cell invasion and metastasis [3–6]. The CAM model has many benefits, such as the highly vascularized nature of the CAM greatly promotes the adeptness of tumor cell grafting, high reproducibility; simplicity and cost effectiveness makes CAM assay a most suitable model for angiogenesis and metastasis studies [4,7].

We used molecular field mapping and alignment approach to design triazine and pyrrolidin-2-one derivatives. Biological targets do not recognize a drug's structure make up. The interaction between a ligand and a protein involves electrostatic fields and surface properties (molecular field). The molecular field description of a compound comprises four fields: positive and negative electrostatic, van der Waals attractive and hydrophobic fields. These fields provide a means of finding the most biologically relevant regions of a molecule, where interactions with a protein are most likely to occur. The Field technology is based on the assumption that two molecules that bind to the same protein site would be expected to have the same field pattern in their bound conformation. Field mapping showed that triazine and pyrrolidin-2-one have field similarity with SU4312 more than 65% (Figure 1). These findings encourage us to synthesize novel triazine and pyrrolidin-2-one derivatives. All the synthesized compounds were screened for anti-angiogenic activity in CAM assay and most active derivatives were analyzed for MCF-7 cell induced anti-angiogenic activity and tumor invasion and metastasis inhibition.

MATERIALS AND METHODS

Chemistry

All the chemicals used were of laboratory grade and procured from Fisher Scientific, S.D. Fine Chemicals and CDH. Melting points were determined by open tube capillary method and are uncorrected. Thin layer chromatography (TLC) plates (silica gel G) were used to confirm the purity of commercial reagents used, compounds synthesized, and to monitor the reactions as well. Two solvent systems; chloroform: methanol in the ratio 6:4 (for compounds of Scheme 1) and ethylacetate : hexane in the ratio 5:5 (for compounds of Scheme 2) were used to run the TLC. The spots were located under iodine vapors/UV light. IR spectra were obtained on a Shimadzu 8400S FT-IR spectrometer (KBr Pellets). ¹H NMR spectra were recorded on a 300 MHz dpx spectrometer in CDCl₃ using TMS as internal standard. ¹³C NMR spectra were recorded at 100 MHz on BRUKER AMX 400 in CDCl₃. Mass spectra were recorded on an API 3000 LC/MS/MS Q3 (SHIMADZU) spectrometer.

General procedure for the preparation of 1,2,4-triazin-3-amine derivatives

Step 1: 1,2,4-triazin-3-amine (1.0 mol) was dissolved in 20 ml ethanol and transferred into round bottom flask. The mixture was heated on water bath till complete dissolution was achieved. To the resulting mixture, aldehyde (2 mol) was added dropwise, and mixture was refluxed for 4 h. The mixture was cooled; Schiff's base (1) was separated, filtered, dried and recrystallized from chloroform and pet. ether (1:1) to afford yellowish microcrystalline powder.

Step 2: Compound 1 (1 mol) was dissolved in methanol (20 ml) by gentle warming. Sodiumborohydride (0.02 mol) was added and mixture was stirred for 1 h. The mixture was heated to 40 °C for 10-15 min. Methanol was evaporated under reduced pressure. The residue was washed with water, dried, and recrystallized from chloroform and pet. ether (1:1) to afford pale yellow microcrystalline powder of compound 2 (Scheme 1).[7-8]

4-amino-2-(((5,6-dimethyl-1,2,4-triazin-3-yl)amino)methyl)phenol (2a)

Light brown color solid, M.P. 110-112°C, m/z: 245.13 (100.0%), 246.13 (13.2%), 246.12 (1.8%), 247.13 (1.2%) (C₁₂H₁₅N₅O, calc. 245.28); FT-IR (KBr) (cm⁻¹): 3350- 3180 (-CONH- str), 2920.32 (C-H str), 813.77 (para disubstituted benzene), 1560 (C-N- str), 1650 (C=O str), 1286 (-C-N- str), 1450 (-CN bend), 1145 (Ar-CH bend). ¹H NMR (300 MHz) DMSO, δ (ppm): 2.33 (s, 3H), 2.86 (s, 3H), 4.11 (s, 1H), 4.60 (s, 2H), 5.44 (s, 1H), 6.17-6.53 (m, 3H), 6.31 (s, 1H); ¹³C NMR (300 MHz) DMSO, δ (ppm): 17.7, 19.5, 147.9, 158.2, 162.7, 39.9, 146.9, 128.7, 132.9, 117.1, 116.1, 115.9, 140.5. Elemental Analysis: C, 58.76; H, 6.16; N, 28.55; O, 6.52 found: C, 58.15; H, 6.15; N, 28.77; O, 6.51.

2,4-dibromo-6-(((5,6-dimethyl-1,2,4-triazin-3-yl)amino)methyl)phenol (2b)

Brown color solid, M.P. 131-132°C, m/z: 387.94 (100.0%), 385.94 (51.1%), 389.93 (48.4%), 388.94 (13.1%), 386.94 (6.7%), 390.94 (6.4%), 388.93 (1.5%), 389.94 (1.2%), (C₁₂H₁₂Br₂N₄O) Molecular Weight: 388.06.

FT-IR (KBr) (cm⁻¹): 3350 (-NH- str), 2920.32 (C-H str), 650 (C-Br), 1560 (C-N- str), 2902 (C=C str), 1450 (-CN bend), 1145 (Ar-CH bend). ¹HNMR (300 MHz) DMSO, δ (ppm): 2.74 (s, 3H), 2.40 (s, 3H), 4.5 (s, 2H), 7.7-7.8 (m, 1H), 5.49 (s, 1H), 4.9 (s, 1H); ¹³C NMR (300 MHz) DMSO, δ (ppm): 17.7, 19.5, 147.7, 159.5, 162.0, 149.9, 133.8, 38.5, 130.1, 115.1, 131.5, 110.7. Elemental Analysis: C, 37.14; H, 3.12; Br, 41.18; N, 14.44; O, 4.12 found: C, 37.10; H, 3.10; Br, 41.11; N, 14.3; O, 4.02.

2-(((5,6-dimethyl-1,2,4-triazin-3-yl)amino)methyl)-4-methylphenol (2c)

Reddish yellow color solid, M.P. 135-136 °C, m/z: 244.13 (100.0%), 245.14 (14.3%), 245.13 (1.5%), 246.14 (1.2%) (C₁₃H₁₆N₄O, Molecular Weight: 244.29). FT-IR (KBr) (cm⁻¹): 3600 (-OH str), 3350 (-NH- str), 2920.32 (C-H str), 1560 (C-N- str), 2902 (C=C str), 1450 (-CN bend), 1145 (Ar-CH bend). ¹HNMR (300 MHz) DMSO, δ (ppm): 2.74 (s, 3H), 2.34 (d, 6H), 4.5 (s, 2H), 7.1 (s, 1H), 7.21 (s, 1H), 6.92 (s, 1H), 5.49 (s, 1H), 4.2 (s, 1H); ¹³C NMR (300 MHz) DMSO, δ (ppm): 17.7, 19.5, 147.7, 159.5, 162.0, 120.5, 129.4, 130.5, 130.8, 128.9, 153.8, 40.2, 21.9. Elemental Analysis: C, 63.91; H, 6.60; N, 22.93; O, 6.55, found: C, 63.90; H, 6.50; N, 22.90; O, 6.56.

2-(((5,6-dimethyl-1,2,4-triazin-3-yl)amino)methyl)-6-methylphenol (2d)

Reddish yellow color solid, M.P. 141-142 °C, m/z: 244.13 (100.0%), 245.14 (14.3%), 245.13 (1.5%), 246.14 (1.2%) (C₁₃H₁₆N₄O, Molecular Weight: 244.29). FT-IR (KBr) (cm⁻¹): 3600 (-OH str), 3350 (-NH- str), 2920.32 (C-H str), 1560 (C-N- str), 2902 (C=C str), 1450 (-CN bend), 1145 (Ar-CH bend). ¹HNMR (300 MHz) DMSO, δ (ppm): 2.74 (s, 3H), 2.34 (d, 6H), 4.5 (s, 2H), 7.1 (s, 1H), 7.21 (s, 1H), 6.92 (s, 1H), 5.49 (s, 1H), 4.2 (s, 1H); ¹³C NMR (300 MHz) DMSO, δ (ppm): 17.7, 19.5, 147.7, 159.5, 162.0, 120.5, 129.4, 130.5, 130.8, 128.9, 153.8, 40.2, 21.9. Elemental Analysis: C, 63.91; H, 6.60; N, 22.93; O, 6.55, found Elemental Analysis: C, 63.81; H, 6.50; N, 22.83; O, 6.45.

3-(((5,6-dimethyl-1,2,4-triazin-3-yl)amino)methyl)-2-methoxyphenol (2e)

Light yellow color solid, M.P. 151-152 °C, m/z: 232.10 (100.0%), 233.10 (12.1%), 233.09 (1.5%), 234.10 (1.2%) (C₁₁H₁₂N₄O₂, Molecular Weight: 232.24). FT-IR (KBr) (cm⁻¹): 3600 (-OH str), 3350 (-NH- str), 2920.32 (C-H str), 1560 (C-N- str), 2902 (C=C str), 1450 (-CN bend), 1145 (Ar-CH bend). ¹HNMR (300 MHz) DMSO, δ (ppm): 2.34 (s, 3H), 2.84 (s, 3H), 3.93 (s, 3H), 4.5 (s, 2H), 6.82-7.1 (m, 1H), 5.49 (s, 1H), 4.15 (s, 1H). ¹³C NMR (300 MHz) DMSO, δ (ppm): 139.7, 149.5, 162.0, 120.5, 116.4, 147.5, 147.8, 108.9, 133.8, 47.2, 56.9, 19.5, 17.7. Elemental Analysis: C, 56.89; H, 5.21; N, 24.12; O, 13.78 found: C, 56.69; H, 5.11; N, 24.10; O, 13.68.

2-(((1,2,4-triazin-3-yl)amino)methyl)-4-nitrophenol (2f)

Light yellow color solid, M.P. 109-110 °C, m/z: 247.07 (100.0%), 248.07 (12.8%). (C₁₀H₉N₅O₃, Molecular Weight: 247.21). FT-IR (KBr) (cm⁻¹): 3600 (-OH str), 3350 (-NH- str), 2920.32 (C-H str), 1560 (C-N- str), 2902 (C=C str), 1450 (-CN bend), 1145 (Ar-CH bend). ¹HNMR (300 MHz) DMSO, δ (ppm): 8.74 (d, 1H), 8.54 (d, 1H), 3.93 (s, 3H), 4.5 (s, 2H), 7.82-7.90 (m, 2H), 7.1 (d, 1H), 5.49 (s, 1H), 4.15 (s, 1H). ¹³C NMR (300 MHz) DMSO, δ (ppm): 139.7, 149.5, 162.0, 125.5, 127.4, 117.5, 140.8, 130.4, 163.8, 40.1. Elemental Analysis: C, 48.58; H, 3.67; N, 28.33; O, 19.42, Found : C, 48.48; H, 3.63; N, 28.13; O, 19.25

4-(((1,2,4-triazin-3-yl)amino)methyl)-2-methoxyphenol (2g)

Brown color solid, M.P. 120-121 °C, m/z: 232.10 (100.0%), 233.10 (12.1%), 233.09 (1.5%), 234.10 (1.2%) (C₁₁H₁₂N₄O₂, Molecular Weight: 232.24). FT-IR (KBr) (cm⁻¹): 3600 (-OH str), 3350 (-NH- str), 2920.32 (C-H str), 1560 (C-N- str), 2902 (C=C str), 1450 (-CN bend), 1145 (Ar-CH bend). ¹HNMR (300 MHz) DMSO, δ (ppm): 8.74 (d, 1H), 8.54 (d, 1H), 3.93 (s, 3H), 4.5 (s, 2H), 6.82-7.1 (m, 1H), 5.49 (s, 1H), 4.15 (s, 1H). ¹³C NMR (300 MHz) DMSO, δ (ppm): 139.7, 149.5, 162.0, 120.5, 116.4, 147.5, 147.8, 108.9, 133.8, 47.2, 56.9. Elemental Analysis: C, 56.89; H, 5.21; N, 24.12; O, 13.78 found: C, 55.89; H, 5.01; N, 24.09; O, 13.51.

2-(((1,2,4-triazin-3-yl)amino)methyl)-4,6-dibromophenol (2h)

Reddish yellow color solid, M.P. 109-110 °C, m/z: 359.90 (100.0%), 357.91 (51.4%), 361.90 (48.8%), 360.91 (11.0%), 358.91 (5.6%), 362.91 (5.4%), 360.90 (1.5%). (C₁₀H₈Br₂N₄O, Molecular Weight: 360.00). FT-IR (KBr) (cm⁻¹): 3600 (-OH str), 3350 (-NH- str), 2920.32 (C-H str), 1560 (C-N- str), 2902 (C=C str), 1450 (-CN bend), 1145 (Ar-CH bend). ¹HNMR (300 MHz) DMSO, δ (ppm): 8.74 (d, 1H), 8.50 (d, 1H), 4.5 (s, 2H), 7.8 (s, 1H), 7.61 (s, 1H), 5.49 (s, 1H), 4.1 (s, 1H). ¹³C NMR (300 MHz) DMSO, δ (ppm): 139.7, 149.5, 162.0, 149.9, 133.8, 38.5, 130.1, 115.1, 131.5, 110.7. Elemental Analysis: Calcd. C, 33.36; H, 2.24; Br, 44.39; N, 15.56; O, 4.44; found: C, 33.11; H, 2.21; Br, 43.99; N, 15.16; O, 4.64.

2-((1,2,4-triazin-3-yl)amino)methyl-4-methoxyphenol (2i)

Reddish yellow color solid, M.P. 101-103 °C, m/z: 232.10 (100.0%), 233.10 (12.1%), 233.09 (1.5%), 234.10 (1.2%). (C₁₁H₁₂N₄O₂, Molecular Weight: 232.24). FT-IR (KBr) (cm⁻¹): 3600 (-OH str), 3350 (-NH- str), 2920.32 (C-H str), 1560 (C-N - str), 2902 (C=C str), 1450 (-CN bend), 1145 (Ar-CH bend). ¹HNMR (300 MHz) DMSO, δ (ppm): 8.74 (d, 1H), 8.54 (d, 1H), 3.93 (s, 3H), 4.5 (s, 2H), 7.1 (s, 1H), 6.99 (s, 1H), 6.82 (s, 1H), 5.49 (s, 1H), 4.15 (s, 1H). ¹³C NMR (300 MHz) DMSO, δ (ppm): 139.7, 149.5, 162.0, 129.5, 116.4, 155.5, 147.8, 113.9, 112.9, 47.2, 56.9. Elemental Analysis: C, 56.89; H, 5.21; N, 24.12; O, 13.78; found: C, 56.81; H, 5.22; N, 24.10; O, 13.18.

2-((1,2,4-triazin-3-yl)amino)methyl-6-methylphenol (2j)

Yellow color solid, M.P. 103-105 °C, m/z: 216.10 (100.0%), 217.10 (13.4%). (C₁₁H₁₂N₄O, Molecular Weight: 216.24). FT-IR (KBr) (cm⁻¹): 3600 (-OH str), 3350 (-NH- str), 2920.32 (C-H str), 1560 (C-N - str), 2902 (C=C str), 1450 (-CN bend), 1145 (Ar C-H bend). ¹HNMR (300 MHz) DMSO, δ (ppm): 8.72 (s, 1H), 8.54 (s, 1H), 2.23 (s, 3H), 4.5 (s, 2H), 6.82-7.1 (m, 1H), 5.49 (s, 1H), 4.15 (s, 1H). ¹³C NMR (300 MHz) DMSO, δ (ppm): 139.7, 149.5, 162.0, 123.5, 130.4, 153.5, 121.2, 128.9, 125.9, 45.2, 15.9. Elemental Analysis: C, 61.10; H, 5.59; N, 25.91; O, 7.40 found: C, 60.95; H, 5.51; N, 25.51; O, 7.39.

General procedure for the preparation of 2-(2-oxopyrrolidin-1-yl)acetamide derivatives

Step 1:

2-(2-oxopyrrolidin-1-yl) acetamide (1.0 mol) was dissolved in 20 ml ethanol and transferred into round bottom flask. The mixture was heated on water bath till complete dissolution was achieved. To the resulting mixture, aldehyde (2.0 mol) was added dropwise, and mixture was refluxed for 4 h. The mixture was cooled; Schiff's base (3) was separated, filtered, dried and recrystallized from chloroform and pet. ether (1:1) to afford microcrystalline powder.

Step 2:

Compound 1 (1 mol) was dissolved in methanol (20 ml) by gentle warming. Sodium borohydride (0.02 mol) was added and mixture was stirred for 1 h. The mixture was heated to 40 °C for 10-15 min. Methanol was evaporated under reduced pressure. The residue was washed with water, dried, and recrystallized from chloroform and pet. ether (1:1) to afford microcrystalline powder of compound 4a-4d (Scheme 2).^[6,7]

N-(2-hydroxy-5-nitrobenzyl)-2-(2-oxopyrrolidin-1-yl)acetamide (4a)

Reddish brown color solid, M.P. 140-141 °C, m/z: 293.10 (100.0%), 294.10 (15.2%), 295.11 (2.0%). (C₁₃H₁₅N₃O₅, Molecular Weight: 293.28). FT-IR (KBr) (cm⁻¹): 3600 (-OH str), 3350 (-NH- str), 2920.32 (C-H str), 1560 (C-N - str), 2902 (C=C str), 1450 (-CN bend), 1145 (Ar C-H bend). ¹HNMR (300 MHz) DMSO, δ (ppm): 7.90-7.95 (m, 2H), 7.19 (d, 1H), 5.45 (s, 1H), 4.47 (s, 2H), 8.013 (s, 1H), 4.51 (s, 1H), 3.35 (t, 2H), 1.80 (p, 2H), 2.35 (t, 2H). ¹³C NMR (300 MHz) DMSO, δ (ppm): 30.3, 17.0, 47.9, 173.7, 55.5, 171.0, 36.1, 129.8, 124.7, 140.3, 127.1, 115.4, 162.7. Elemental Analysis: C, 53.24; H, 5.16; N, 14.33; O, 27.28; found: C, 53.14; H, 5.06; N, 14.13; O, 27.08.

N-(3,5-dibromo-2-hydroxybenzyl)-2-(2-oxopyrrolidin-1-yl)acetamide (4b)

Pale white color solid, M.P. 143-144 °C, m/z: 405.94 (100.0%), 403.94 (51.0%), 407.93 (48.2%), 406.94 (14.3%), 404.94 (7.3%), 408.94 (7.0%), 407.94 (1.7%). (C₁₃H₁₄Br₂N₂O₃, Molecular Weight: 406.07). FT-IR (KBr) (cm⁻¹): 3600 (-OH str), 3350 (-NH- str), 2920.32 (C-H str), 1560 (C-N - str), 2902 (C=C str), 1450 (-CN bend), 1145 (Ar C-H bend). ¹HNMR (300 MHz) DMSO, δ (ppm): 7.54 (s, 1H), 7.76 (s, 1H), 5.35 (s, 1H), 4.47 (s, 2H), 8.03 (t, 1H), 4.58 (s, 1H), 3.32 (t, 2H), 1.99 (p, 2H), 2.35 (t, 2H). ¹³C NMR (300 MHz) DMSO, δ (ppm): 30.3, 17.0, 47.9, 173.7, 55.5, 171.0, 37.1, 129.8, 135.7, 110.9, 132.1, 119.8, 149.8. Elemental Analysis: C, 38.45; H, 3.48; Br, 39.35; N, 6.90; O, 11.82, found: C, 38.35; H, 3.38; Br, 39.15; N, 6.90; O, 11.62.

N-(2-hydroxybenzyl)-2-(2-oxopyrrolidin-1-yl)acetamide (4c)

Reddish color solid, M.P. 135-137°C, m/z: 248.12 (100.0%), 249.12 (14.4%), 250.12 (1.7%). (C₁₃H₁₆N₂O₃, Molecular Weight: 248.28). FT-IR (KBr) (cm⁻¹): 3600 (-OH str), 3350 (-NH- str), 2920.32 (C-H str), 1560 (C-N - str), 2902 (C=C str), 1450 (-CN bend), 1145 (Ar C-H bend). ¹HNMR (300 MHz) DMSO, δ (ppm): 6.51-6.53 (m, 2H), 6.76 (d, 1H), 3.89 (s, 3H), 5.35 (s, 1H), 4.47 (s, 2H), 8.03 (t, 1H), 4.58 (s, 1H), 3.32 (t, 2H), 1.99 (p, 2H), 2.35 (t, 2H). ¹³C NMR (300 MHz) DMSO, δ (ppm): 30.3, 17.0, 47.9, 173.7, 55.5, 171.0, 37.1, 129.8, 143.7, 120.6, 122.1, 109.8, 148.7, 56.1. Elemental Analysis: C, 62.89; H, 6.50; N, 11.28; O, 19.33 found: C, 62.50; H, 6.41; N, 11.28; O, 19.13.

N-(2-hydroxy-3-methoxybenzyl)-2-(2-oxopyrrolidin-1-yl)acetamide (4d)

Yellowish white color solid, M.P. 141-142°C, m/z: 278.13 (100.0%), 279.13 (15.5%), 280.13 (2.0%). (C₁₄H₁₈N₂O₄, Molecular Weight: 278.30). FT-IR (KBr) (cm⁻¹): 3600 (-OH str), 3350 (-NH- str), 2920.32 (C-H str), 1560 (C-N - str), 2902 (C=C str), 1450 (-CN bend), 1145 (Ar C-H bend). ¹HNMR (300 MHz) DMSO, δ (ppm): 6.62-6.63 (m, 2H), 6.89 (t, 1H), 3.91 (s, 3H), 5.45 (s, 1H), 4.47 (s, 2H), 8.013 (s, 1H), 4.51 (s, 1H), 3.35 (t, 2H), 1.80 (p, 2H), 2.35 (t, 2H). ¹³C NMR (300 MHz) DMSO, δ (ppm): 30.3, 17.0, 47.9, 173.7, 55.5, 171.0, 36.1, 129.8, 144.7, 148.3, 123.1, 125.4, 109.7, 56.1. Elemental Analysis C, 60.42; H, 6.52; N, 10.07; O, 23.00; found: C, 60.24; H, 6.20; N, 10.1; O, 22.90.

Biological activity**Chorioallantoic membrane (CAM) assay**

Fertilized eggs from a local commercial hatchery guaranteeing 95% fertilization of the eggs were purchased. Dirt, feathers and excrement were carefully removed from the eggshells mechanically by dry wiping with paper towels and 70% denatured ethanol. Eggs were kept in the incubator on one side, marking the upper surface. All the eggs were incubated at temperature 37.8 °C, and the humidity at 47%. On development day 3, the eggs were opened under laminar airflow. Opening the eggs at a further developmental stage results in damage to the CAM, as the membrane tends to stick to the shell. An infrared lamp is used to keep the eggs warm during the procedure. To lower the level of the CAM by two ml of albumen was removed through an 18 G needle inserted at the tip of the egg. A semipermeable adhesive film at the marked upper side of the shell was applied in order to prevent spilling of shell particles onto the CAM while cutting the window. A window of 1 cm² in the shell was cut, using a pair of sterile sharp-pointed surgical scissors. The embryo's pulsating heart and adjoining vessels can be observed at the surface of the egg yolk. Remove the non-fertilized eggs or dead embryos. The window was sealed with a semipermeable adhesive film. The eggs were incubated for 72 more hours to have CAM reaching 2 cm in diameter. Subsequently (on day 8), the seal was removed and the discs were placed on the chorioallantoic membrane of each egg. The seal was placed again and the eggs were then incubated for 24 h. The angiogenesis level was evaluated after that period by means of a stereomicroscope, by observing the avascular zone surrounding the disc. Antiangiogenic activity is expressed as a score where 0 = no or weak effect, 1 = medium effect, and 2 = strong effect (capillary free zone is at least twice as large as the pellet). The eggs in which the pellets caused inflammation and embryo toxicity were excluded. Furthermore, most active anti-angiogenic derivatives were analyzed for MCF-7 cell induced angiogenesis inhibition in a CAM assay. MCF-7 cancer cells (50 µL, 40,000 cells) were loaded on top of uncoated 12 µm ring inserts. The cells were allowed to migrate and invade to the lower chamber for 6 hours. After 6h treated and MCF-7 found to increase the number of newly formed blood vessel branch points compared to phosphate buffered saline (PBS)-treated control group. Each test compound was also analyzed for their ability to inhibit growth of tumor. Each test compound was prepared in stock solution and diluted with PBS in a concentration of 1.0 µM. 10 µL of this solution was added directly to the disk on top of CAM. Since we measured the blood vessels in the area under the disk, the antiangiogenic dose was calculated as 10 µL/CAM drug concentration (1.0 µM), i.e. 0.01 nmol/CAM. [8-12] (Figure 2)

Cell culture

MCF-7 cell line was obtained from NCCS Pune. The cell line was maintained in monolayer cultures in supplemented Dulbecco's modified eagle's medium (DMEM) with 10 % heat-inactivated fetal bovine serum (FBS), 1 % L-glutamine, and 50 lg/ml gentamycin sulfate, at 37 °C, in CO₂ incubator in an atmosphere of humidified 5 % CO₂ and 95 % air.

Immunohistochemistry

CAM paraffin sections (6 µm) were incubated at 60 °C for 2 hours. Tissue sections were dewaxed with xylene and ethanol, followed by PBS washes. Immunoreactivity was detected using diaminobenzidine/H₂O₂ substrate (Sigma-Aldrich). The sections were counterstained with 10% eosin (Sigma-Aldrich), dehydrated and mounted in Pertex (Medite Medizintechnik, Germany). Slides were digitally scanned using the NanoZoomer (Hamamatsu Photonics K.K.). For quantitative analysis of ovarian cancer cell invasion into the mesoderm layer, 8 to 12 CAM images from each embryo were assessed by two independent researchers.

Molecular modeling

Molecular field mapping and alignment studies were performed using Forge V 10, Cresset software. The receptor model was built by using AutoDock Tools 1.4.6 and MGL Tools 1.5.4 packages. Gasteiger partial charges were added to the ligand atoms. Non-polar hydrogen atoms were merged, and rotatable bonds were defined. Docking

calculations were carried out on 1OHV protein model. Essential hydrogen atoms, Kollman united atom type charges, and solvation parameters were added with the aid of AutoDock tools. Affinity (grid) maps of $xx \text{ \AA}^{\circ}$ grid points and $0.375 \text{ \AA}^{\circ}$ spacing were generated using the Autogrid program. AutoDock parameter set- and distance-dependent dielectric functions were used in the calculation of the van der Waals and the electrostatic terms, respectively. Docking simulations were performed using the Lamarckian genetic algorithm (LGA) and the Solis & Wets local search method. Initial position, orientation, and torsions of the ligand molecules were set randomly. All rotatable torsions were released during docking. Each docking experiment was set to terminate after a maximum of 250,000 energy evaluations. The population size was set to 150. During the search, a translational step of 0.2 \AA° , and quaternion and torsion steps of 5 were applied. [13-16]

RESULTS AND DISCUSSION

Primarily, we performed field analysis of the designed compounds and compared with known antiangiogenic compound SU4312. The field point pattern is a sophisticated 'pharmacophore' which can be used to define a template for binding. Molecules can be overlaid using their fields, rather than structure, and the field similarity between two molecules can be quantified and converted to a similarity value. This is anticipated that compounds having similar arrangement of field points bind to the receptor in similar fashion and affinity. Four molecular fields to represent the binding properties of a ligand are positive electrostatic (colored red), negative electrostatic (colored blue), Van der Waals attractive i.e. 'steric' (colored yellow), hydrophobic (colored orange). Compounds owning field similarity more than 65% with field of reference SU4312 were selected for synthesis. The physical and field similarity data of these compounds are presented in Table 1. The syntheses of triazine and pyrrodine-2-one derivatives (2a-2h and 4a-4d) are outlined in scheme 1 and 2. 3, 5 substituted salicylaldehyde on reaction with 3-amino-1,2,4 triazine or pyrrodine-2-one acetamide, in ethanol, at $60-70^{\circ}\text{C}$ yielded corresponding Schiff bases which, in the presence of sodiumborohydride, were reduced to corresponding amines. Reaction progress was monitored by thin layer chromatography. The ^1H NMR, ^{13}C NMR, IR and mass spectral data of synthesized derivatives were recorded and found in full agreement with the proposed structures. Elemental analysis data confirmed the purity of the compounds.

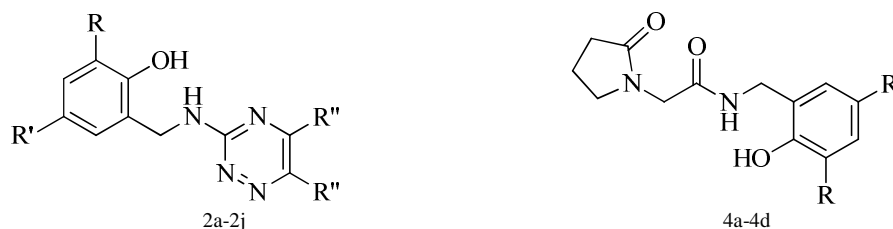
The synthesized compounds were evaluated for anti-angiogenic potential using *in-ovo* CAM assay (Figure 3). The chick immune system does not begin to develop to function until about 2 weeks into its development and can be used for transplantation from various tissues without immune response. Chicken eggs in the early phase of breeding are between *in vitro* and *in vivo* systems and provide a vascular test environment not only to study angiogenesis but also to study tumorigenesis. In addition to nurturing developing allo- and xenografts, the CAM blood vessel network provides a uniquely supportive environment for tumor cell intravasation, dissemination, and vascular arrest and a repository where arrested cells extravasate to form micro metastatic foci. Test compounds, at the fixed concentration 0.01nm , soaked in a disk were used for CAM assay. SU4312 compound was used as reference for comparison. All the results are depicted in Table 2. Derivative 2b, 2c and 4d were found most potent during the angiogenic assay and further analyzed for MCF-7 cell induced angiogenesis in a CAM assay. Derivative 2b, 2c and 4d are found to have anti-angiogenic activity score 1.9, 1.8 and 1.8 respectively which is comparable with reference anti-angiogenic score 1.91. Further it was observed that molecules 2b, 2c and 4d inhibit tumor cell induced angiogenesis and tumor growth significantly Figure 4. Figure 4 displays Inhibition of angiogenesis which reveals that small blood vessels network serve role as nutrition shipper for the tumor and their inhibition leads to retardation in tumor growth. Molecule 2b (Figure 4B) was found more effective with less tumor growth. The immunostaining of transverse sections (Figure 5) of CAM also performed and (a) Control shows the normal structure of the CAM layers; ectoderm (ET), mesoderm (M) and endoderm (ED); (b) figure showing cell grafts (CG) were placed on top of the ectoderm layer and cancer cell invasion into the CAM mesoderm was assessed in day 14 chick embryos. (c) Figure showing growth of cancer after treatment with compound 2b.

The molecular docking was performed into the hydrophobic site of VEGFR (Pdb: 3nlv) with the aim to predict anti-angiogenic activity of the most active compounds of the study (compounds 2b, 2c and 4d) (Figure 5). The complexes were energy-minimized with a MMFF94 force field till the gradient convergence 0.01 kcal/mol was reached (Table 3). Compound 2b exhibited hydrophobic interactions; PRO-682 (-0.07 \AA), MET-589 (-0.06 \AA), TRP-678 (-0.06 \AA), TRP-676 (1.2 \AA); Hydrogen bonding with VAL-670 (-5.8 \AA), VAL-680 (-1.9 \AA), PRO-681(0.02). Compound 2c exhibited hydrophobic interactions; PRO-682 (-0.75 \AA), TRP-676 (-0.75 \AA); hydrogen bonding with TRP-678 (-0.7), VAL-680 (-0.5 \AA), VAL-677 (-0.1 \AA). Compound 4d displayed hydrophobic interactions, PRO-682 (-0.07 \AA), MET-589 (-0.06 \AA), TRP-678 (-0.06 \AA), TRP-676 (1.2 \AA); hydrogen bonding with VAL-670 (-5.8 \AA),

VAL-680 (-1.9 Å), PRO-681(0.02). Reference SU4312 showed hydrophobic interactions, PRO-682 (-1.4 Å), TRP-678 (-1.9Å), Hydrogen bonding with VAL-677 (-0.2Å), VAL-680 (-0.3 Å) (Figure 6).

The NH-bridge between to moiety is essential for hydrogen bonding with protein. Electronegative atom substitution in phenol moiety leads to increase in activity due to increase in hydrophobic interaction with protein and coplanarity.

Table 1: Physical properties of the synthesized derivatives



Code	R	R'	R''	Molecular formula	slogP	Similarity value	MW	M.P (°C)	Rf	(%) Yield
2a	H	NH ₂	CH ₃	C ₁₂ H ₁₃ N ₅ O	1.3	0.726	243.3	130-131	0.7	65
2b	Br	Br	CH ₃	C ₁₂ H ₁₂ N ₄ OBr ₂	3.5	0.759	388.1	131-132	0.59	68
2c	H	CH ₃	CH ₃	C ₁₃ H ₁₆ N ₄ O	2.1	0.739	244.3	135-136	0.6	75
2d	CH ₃	-	CH ₃	C ₁₃ H ₁₆ N ₄ O	2.1	0.737	244.3	141-142	0.46	76
2e	4-OH	5-OCH ₃	CH ₃	C ₁₃ H ₁₆ N ₄ O ₂	1.8	0.791	260.3	151-152	0.8	42
2f	H	NO ₂	H	C ₁₀ H ₉ N ₅ O ₃	1.0	0.671	247.2	109-110	0.7	70
2g	4-OH	5-OCH ₃	H	C ₁₁ H ₁₂ N ₄ O ₂	1.2	0.709	232.2	120-121	0.72	74
2h	Br	Br	H	C ₁₀ H ₈ N ₄ OBr ₂	2.9	0.686	360.0	109-03	0.63	55
2i	H	-OCH ₃	H	C ₁₁ H ₁₂ N ₄ O ₂	1.2	0.686	232.2	101-103	0.65	54
2j	CH ₃	H	H	C ₁₁ H ₁₂ N ₄ O	1.5	0.69	216.2	103-105	0.45	59
4a	H	NO ₂	-	C ₁₃ H ₁₃ N ₃ O ₃	0.4	0.665	293.3	140-141	0.53	65
4b	Br	Br	-	C ₁₃ H ₁₄ N ₂ O ₃ Br ₂	2.3	0.677	406.1	143-144	0.6	63
4c	H	H	-	C ₁₃ H ₁₆ N ₂ O ₃	0.6	0.694	248.3	135-137	0.75	55
4d	OCH ₃	H	-	C ₁₄ H ₁₈ N ₂ O ₄	0.6	0.684	278.3	141-142	0.65	68
SU4312				C ₁₇ H ₁₆ N ₂ O	3.2		264.3			

Table 2. *in vivo* anti-angiogenic activity of synthesized derivatives

Compounds	Concentration (nm)	Score
2a	0.01	1.4 ± 0.1 (n=3)
2b	0.01	1.9 ± 0.1 (n=3)
2c	0.01	1.8 ± 0.1 (n=3)
2d	0.01	1.3 ± 0.1 (n=3)
2e	0.01	toxic (n=3)
2f	0.01	1.5 ± 0.1 (n=3)
2g	0.01	toxic (n=3)
2h	0.01	1.5 ± 0.1 (n=3)
2i	0.01	1.3 ± 0.1 (n=3)
2j	0.01	1.4 ± 0.1 (n=3)
4a	0.01	1.4 ± 0.1 (n=3)
4b	0.01	1.3 ± 0.1 (n=3)
4c	0.01	1.5 ± 0.1 (n=3)
4d	0.01	1.8 ± 0.1 (n=3)
SU4312	0.01	1.91 ± 0.1 (n=3)

Table 3: Energy table of active compounds and SU4312

Compound	Est. Free Energy of Binding (kcal/mol)	Est. Inhibition Constant, Ki uM	vdW + Hbond + desolv Energy (kcal/mol)	Electrostatic Energy (kcal/mol)	Total Intermolec. Energy (kcal/mol)	Interact. Surface
2b	-6.63	13.73	-6.97	-0.20	-7.17	538.45
2c	-7.14	5.81	-7.62	-0.11	-7.73	591.08
4d	-6.01	39.51	-6.73	-0.24	-6.97	574.35
SU4312	-6.84	9.66	-7.37	-0.06	-7.43	634.77

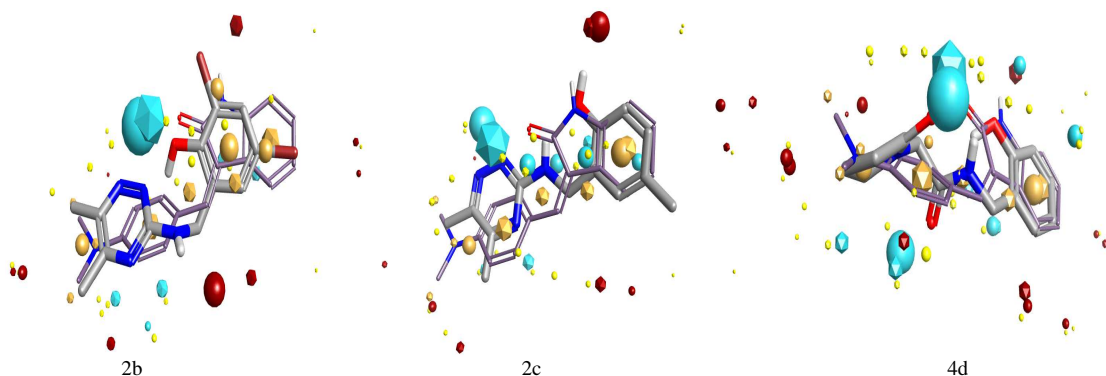
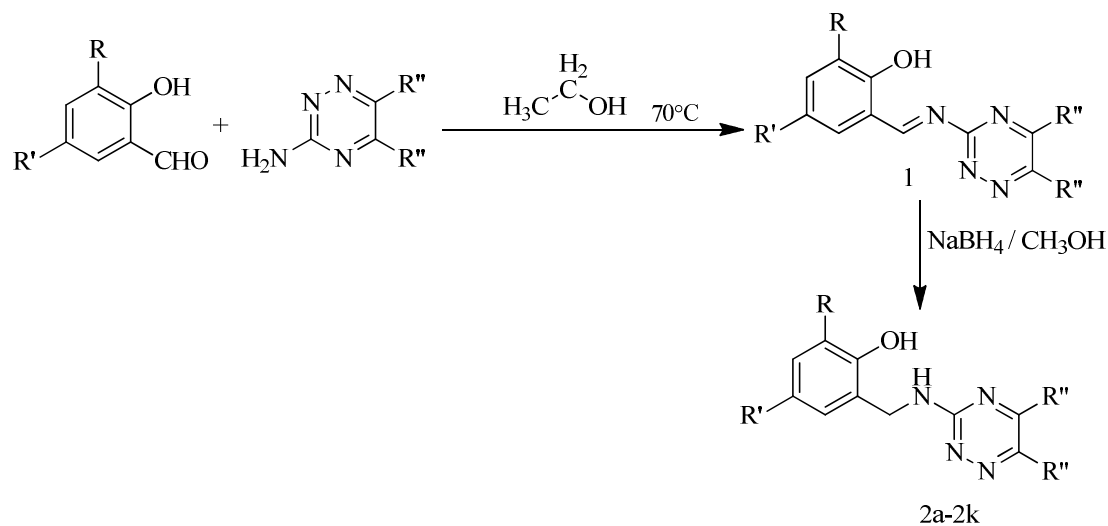
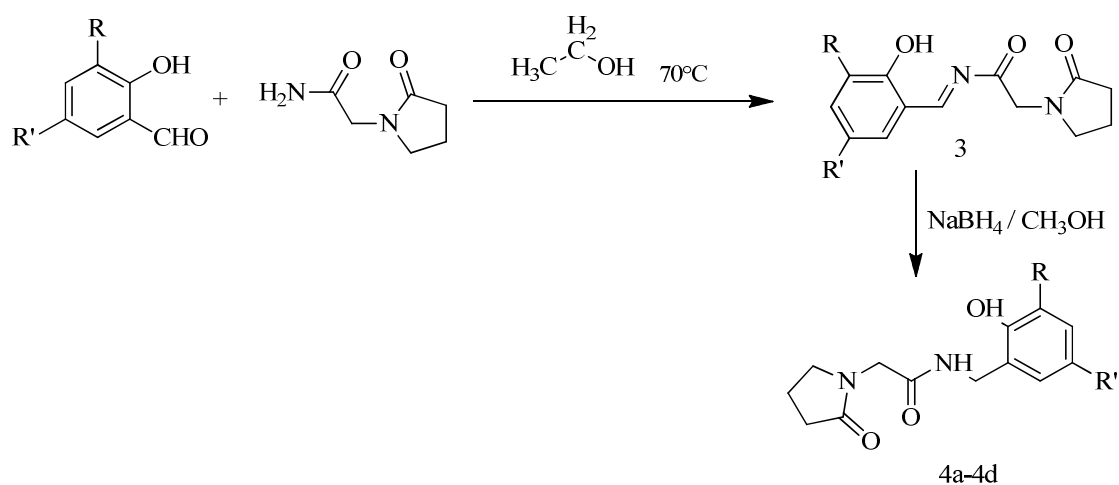


Figure 1. Field point alignment of the most active synthesized derivatives. The size of the point indicates the potential strength of the interaction. Round-shaped field points are of test 2b, 2c and 4d. Diamond-shaped field points are of reference compound (SU4312). Sky blue color: negative ionic fields; magenta color: positive ionic fields; light yellow color: Vander waal interactions; dark yellow color: hydrophobic fields. Field similarity score, 2b: 0.759; 2c: 0.739; 4d: 0.699



Scheme 1. Synthesis route of triazine derivatives



Scheme 2. Synthesis route of pyrrolidine-2-one derivatives

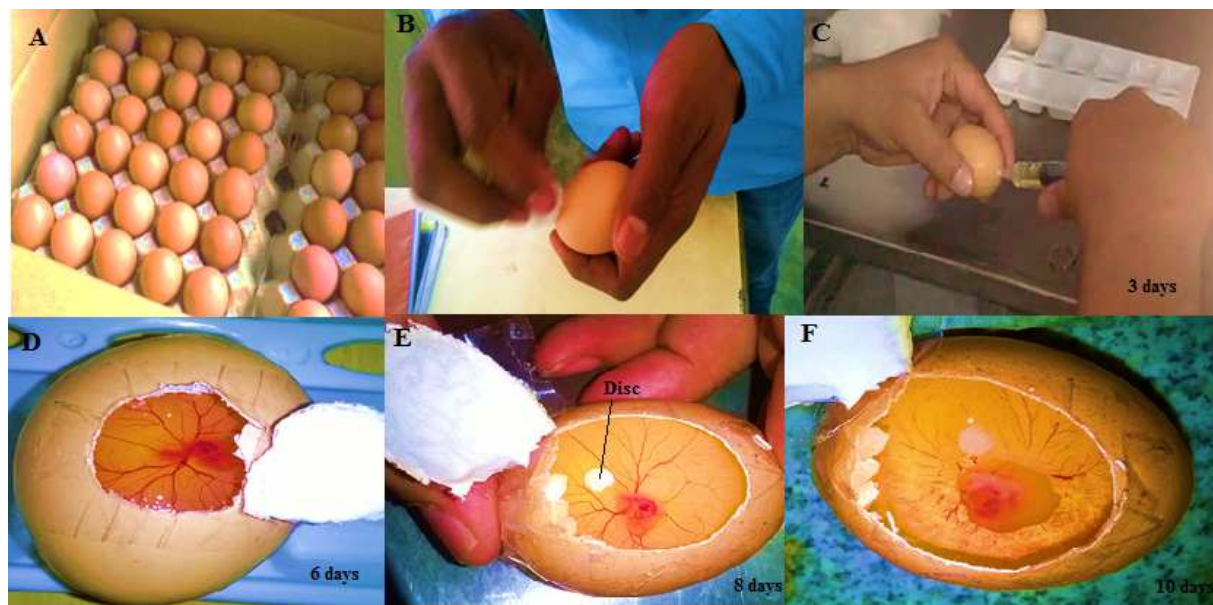


Figure 2. CAM assay. A: Fertilized eggs were purchased from local market. B: Eggs shells were cleaned with ethanol. C: after three days incubation 2-3 ml egg white was taken out to lower the CAM. D: 6 days CAM, E: Placement of Disc Soaked with test sample, F: Angiogenesis inhibition

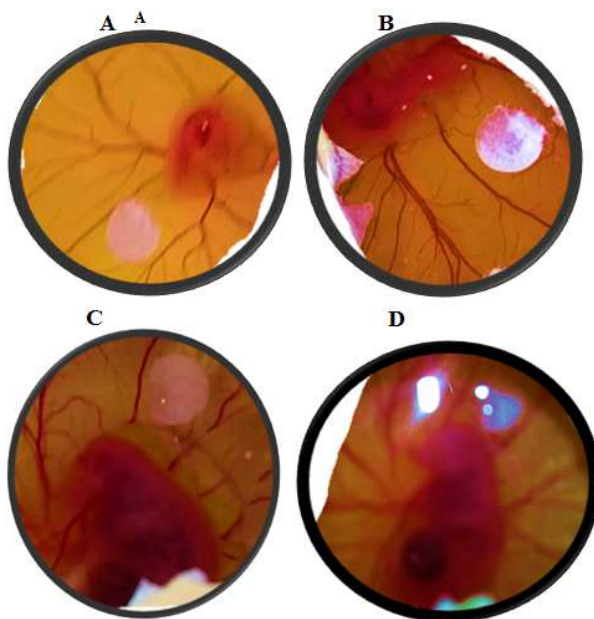


Figure 3: Anti-angiogenesis of compound reference, 2b, 2c and 4d respectively

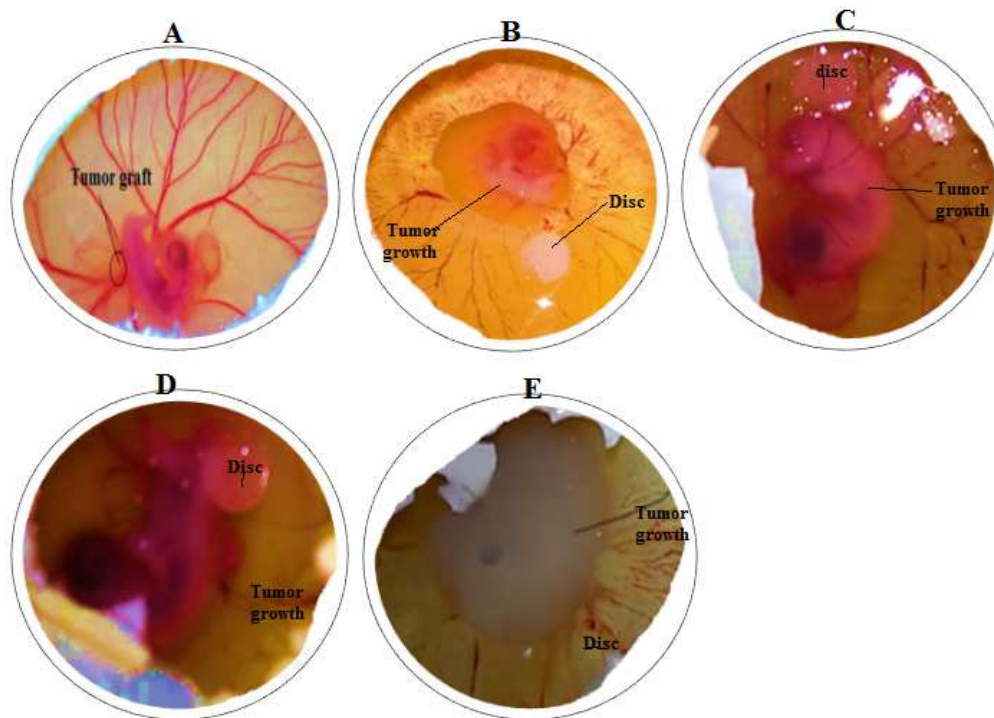


Figure 4. MCF-7 cells induced angiogenesis and metastasis inhibition. A. Showing MCF-7 cells graft on CAM. B, C, D, E Showing angiogenesis inhibition and tumor growth of 2b, 2c, 4d and phosphate buffer respectively

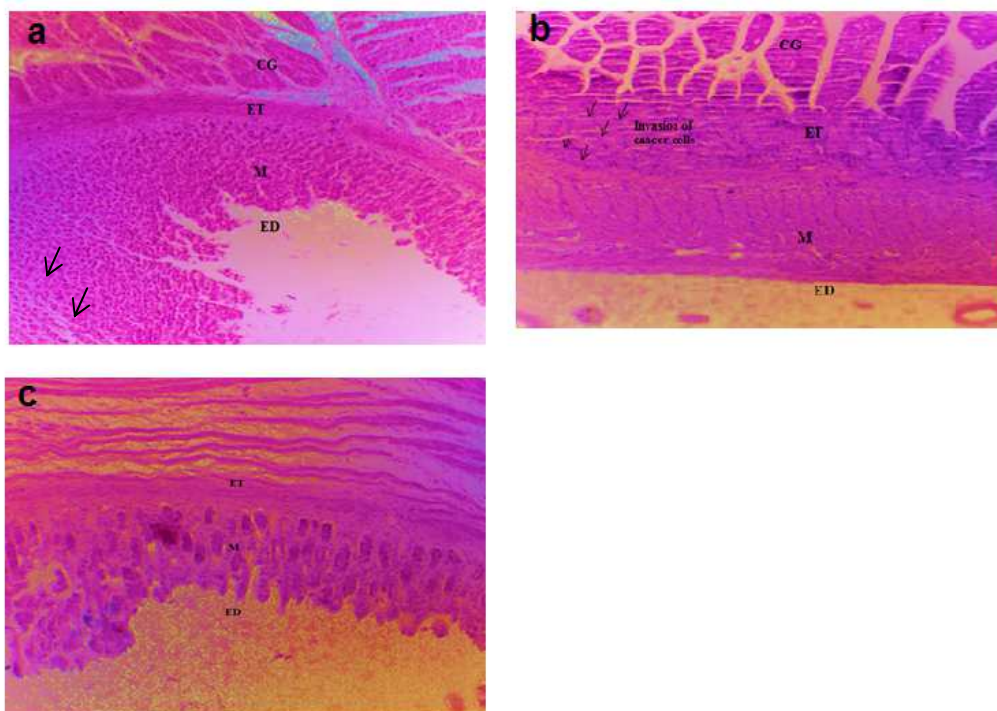
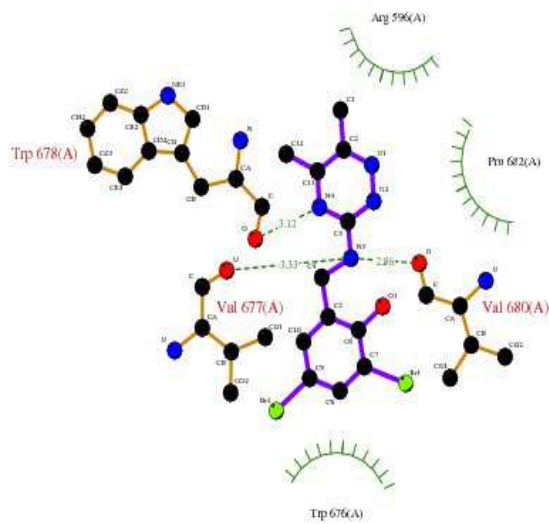
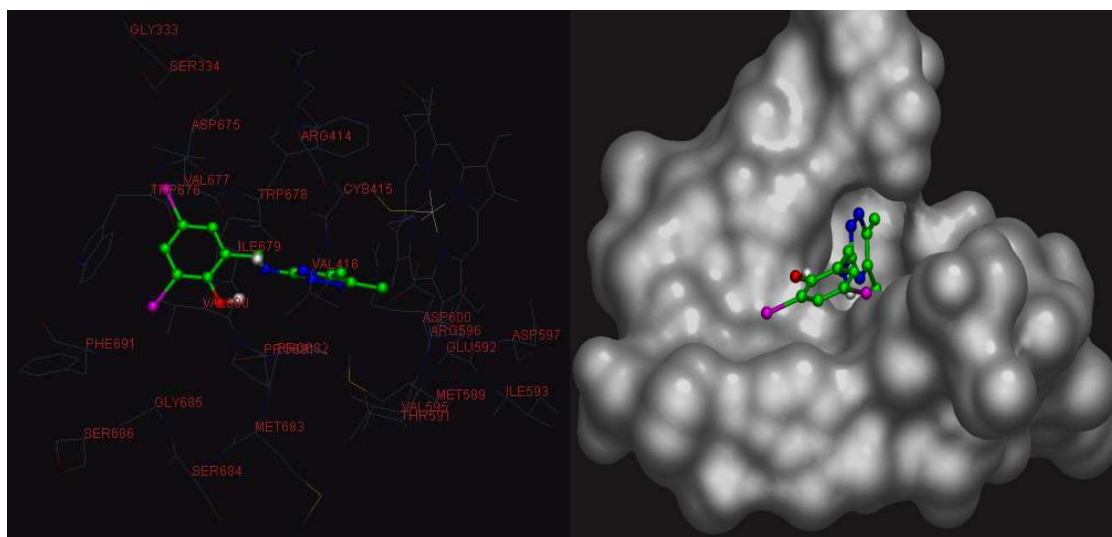


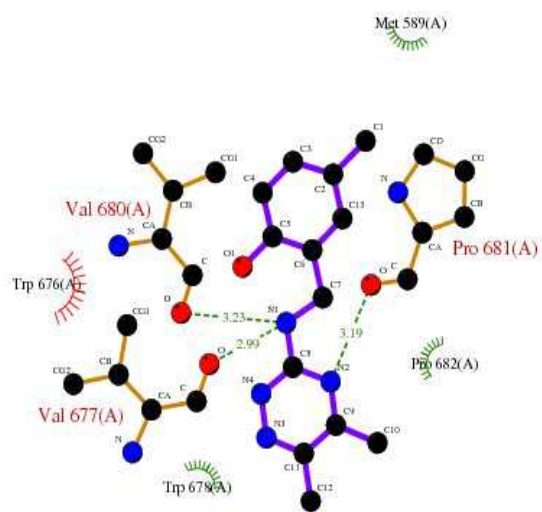
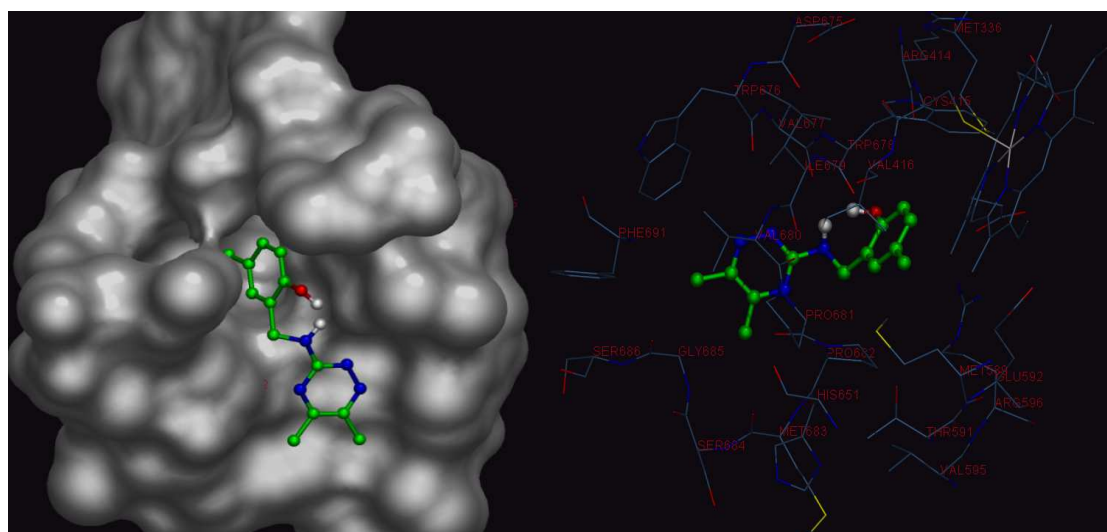
Figure 5. (a) Control showing the normal structure of the CAM layers; ectoderm (ET), mesoderm (M) and endoderm (ED); (b) figure showing cell grafts (CG) were placed on top of the ectoderm layer and cancer cell invasion into the CAM mesoderm was assessed in day 14 chick embryos. (c) Figure showing growth of cancer after treatment with compound CAM paraffin sections (6 μ m) were stained. Original magnification $\times 200$, scale bar 100 μ m

Figure 6. Docking of compounds into the active site of vascular epidermal growth factor receptor pdb: 3nlv

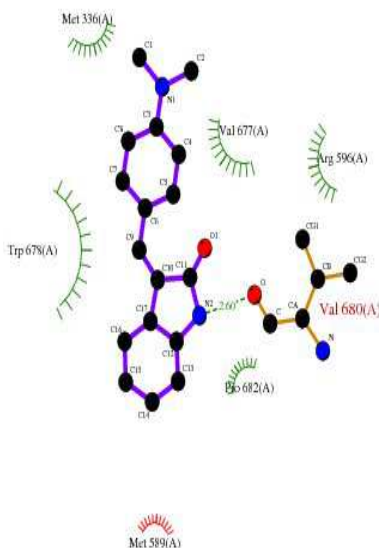
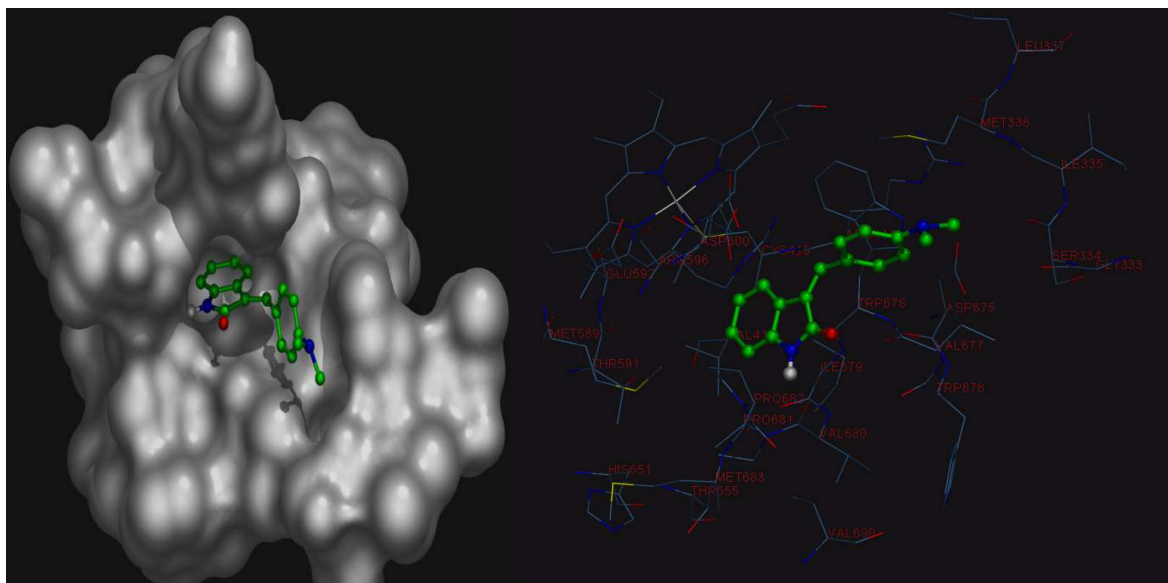
2b



2c



SU4312



CONCLUSION

Cancer cells grow and divide much more rapidly than normal cells; they have a much higher demand for nutrients and oxygen. Increase in blood vessels numbers is to complete the demand of nutrients. Inhibition of angiogenesis leads to cut off nutrient supplier and can inhibit cancer growth by starving them. Two series of triazine and pyrrolidin-2-one derivatives were synthesized in order to obtain new compounds with potential anti-angiogenic activity. All compounds were evaluated for their anti-angiogenic activity by chorioallantoic membrane (CAM) assay method. Compound 2b, 2c and 3d showed maximum activity out of all synthesized compounds. Molecule 2b was found to inhibit MCF-7 cells induced angiogenesis and their growth significantly. Molecular docking studies of most active compounds of the series revealed that they interact with narrow hydrophobic pocket of the N-terminal chain in the ATP binding site of VEGFR. These results reveal that angiogenesis is a nutrient supplier for tumor and inhibition of blood vessels leads to retardation of the tumor growth.

Acknowledgments

The authors are thankful NCCS Pune and Cresset group for the support during the study. Authors are especially thankful to Arjun, Sanjay and Kapil, Lab Assistant S V Subharti University for their valuable support.

REFERENCES

- [1] <https://www.angiorg/learn/angiogenesis>accessed on 05.01.2016
- [2] N Ferrara, RS Kerbel, *Nature*, **2005**, 438, 967-974.
- [3] P Carmeliet, *Nature*, **2005**, 438, 932-936.
- [4] R Kumar, TS Sirohi, H Singh *et al*, *Mini Rev Med Chem*, **2014**, 14,168-207.
- [5] J Zhang, X Pan , C Wang *et al*, *Chem Biol Drug Des*, **2012**, 79, 353-363.
- [6] F Bellina, R Rossi, *Tetrahedron*, **2006**, 62, 7213-7256.
- [7] V Garg, A Kumar, A Chaudhary, S Agrawal *et al*, *Med Chem Res*, **2013**, 22, 5256-5266.
- [8] DS Dohle, SD Pasa, S Gustmann, M Laub *et al*, *J Visualized Experiments*, **2009**, 3-6.
- [9] D Ribatti, *Experimntal cell Res*, **2014**, 328, 314-324.
- [10] NK Lokman, ASF Elder, C Ricciardelli *et al*, *Int J Mol Sci*, **2012**, 13, 9959-9970.
- [11] M Hagedorn, S Javerzat, D Gilges *et al*, *Proceedings of the Natl Acad Sci USA*, **2005**, 102, 1643-1648
- [12] EI Deryugina, PJ Quigley, *Histochem Cell Biol*, **2008**, 130, 1119-1130.
- [13] Z Bikadi, E Hazai, *J Cheminf*, **2009**, 1, 1-16.
- [14] TA Halgren, *J Comp Chem*, **1998**, 17, 490-519.
- [15] GM Morris, DS Goodsell, AJ Olson, *J Comp Chem*, **1998**, 19, 1639-1662.
- [16] FJ Solis, RJB Wets, *Math Method Oper Res*, **1981**, 6, 19-30.